Supplementary Materials

Facile Synthesis of Bismuth Oxide/Bismuth Vanadate Heterostructures for Efficient Photoelectrochemical Water Splitting

Kai-Hang Ye,[a] Xiang Yu,[ab] Zhiguang Qiu,[a] Yi Zhu,[a] Xihong Lu[c] and Yuanming Zhang [a,*]

[a] Department of Chemistry, Jinan University, Guangzhou 510632, People's Republic China; E-mail: tzhangym@jnu.edu.cn Tel: +86-20-85222756; Fax: +86-20-85222756

[b] Analytic and Testing Centre, Jinan University, Guangzhou, China 510632.

[c] MOE of the Key Laboratory of Bioinorganic and Synthetic Chemistry, KLGHEI of Environment and Energy Chemistry, School of Chemistry and Chemical Engineering, Sun Yat-Sen University, Guangzhou 510275

Experimental

Photocatalysts preparation

The fabrication process of $Bi_2O_3/BiVO_4$ heterostructures involves two processes, as shown in Figure 1. Firstly, the Bi nanobelts were grown on a FTO substrate by a template-free electrochemical deposition. In general, a piece of FTO (around 2.0 cm^2) served as the working electrode, a Pt electrode as the counter electrode and an Ag/AgCl electrode as the reference electrode. Cathodic electrodeposition was performed at a constant current of 2 mA cm^{-2} at 60 ^oC in solutions containing 0.005 mol L^{-1} $Bi(NO_3)_3$, 0.05 mol L^{-1} ethylenediamine tetraacetic acid disodium (Na_2EDTA) and 0.1 mol L^{-1} sucrose. The second step was the conversion of Bi to Bi_2O_3/

$BiVO_4$ heterostructures, which was achieved by impregnating Bi electrodes in the solution of 0.1 mol L^{-1} NH_4VO_3 for 3 h, 6 h, and 12 h, followed by annealing in air at 550 ^oC for 6 h to prepare $Bi_2O_3/BiVO_4$ heterostructures and pure $BiVO_4$. At last, the annealed electrodes were soaked into 1 mol L^{-1} KOH for 1 h to remove the excess V_2O_5. On the other hand, Bi electrodes were annealed in air at 550 ^oC without impregnating. In comparison, pure Bi_2O_3 was also synthesis by directly calcined the as-prepared Bi nanobelts in air.

In the presence of the air, the Bi and NH_4VO_3 can reacted with the oxygen under heating conditions:

$$2Bi + 2NH_4VO_3 + O_2 \rightarrow 2BiVO_4 + 2NH_3 + H_2O$$

$$2Bi + 3O_2 \rightarrow 2Bi_2O_3$$

The product can be controlled by controlled the amount of NH_4VO_3 with different immersion times in the NH_4VO_3 solution.

Characterizations and measurements

The morphology, phase and composition of the as-synthesized products were characterized by field emission scanning electron microscope (FE-SEM, JSM-6330F), X-Ray Diffractometer (XRD, D8 ADVANCE), transmission electron microscopy (TEM, JEM2010-HR, FEI Tecnai G^2 F30), X-ray Photoelectron Spectroscopy (XPS, ESCALab250) and Raman spectroscopy (Renishaw inVia). The optical properties of the products were measured with UV-Vis-NIR Spectrophotometer (UV-Vis-NIR, Shimadzu UV-2450).

PEC measurements were carried out in a three-electrode cell with a flat quartz window to facilitate illumination of the photoelectrode surface in 0.1 mol L^{-1} Na_2SO_4 solution. The working electrode is the as-synthesized products, while Pt electrode and Ag/AgCl electrode were used as

counter and reference electrode, respectively. The illumination source was a 300 W Xe arc lamp (PLS-SXE-300/300UV, Beijing Trusttech Co. Ltd.) directed at the quartz photoelectrochemical cell. The intensity of the light is about 100 mW^{-2}. The current densities were recorded with CHI 760D electrochemical workstation (CHI, Shanghai).

Incident-photon-to-current-conversion-efficiency (IPCE) measurements were conducted with a solar simulator (Newport 69911 300 W xenon lamp), coupled to an aligned monochromator (Oriel Cornerstone 260 1/4m). IPCE can be expressed as:

$$IPCE=(1240I)/(\lambda J_{light})$$

Where I is the measured photocurrent density at a specific wavelength, λ is the wavelength of incident light, and J_{light} is the measured irradiance at a specific wavelength. The carrier density was calculated by the following Mott-Schottky equation:

$$N_d = (2/e_0\varepsilon\varepsilon_0)[d(1/C^2)/dV]^{-1}$$

where e_0 is the electron charge, ε the dielectric constant of $BiVO_4$ (ε = ~86) [20], ε_0 the permittivity of vacuum, N_d the dopant density and V the electrode applied potential.

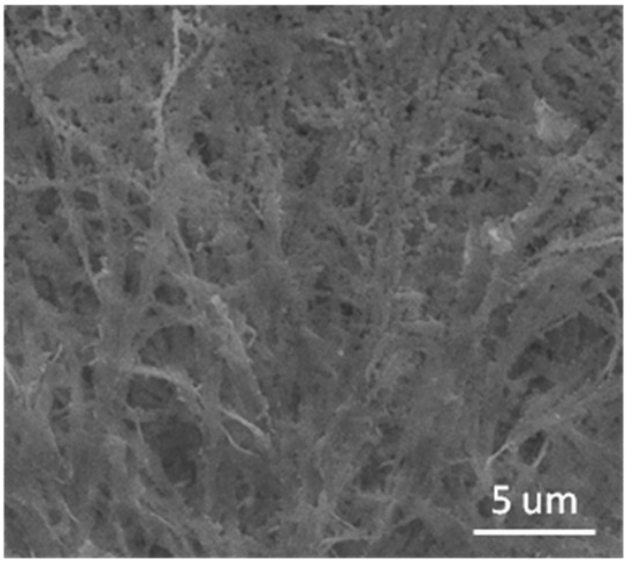

Figure S1. SEM of $Bi_2O_3/BiVO_4$ heterostructures.

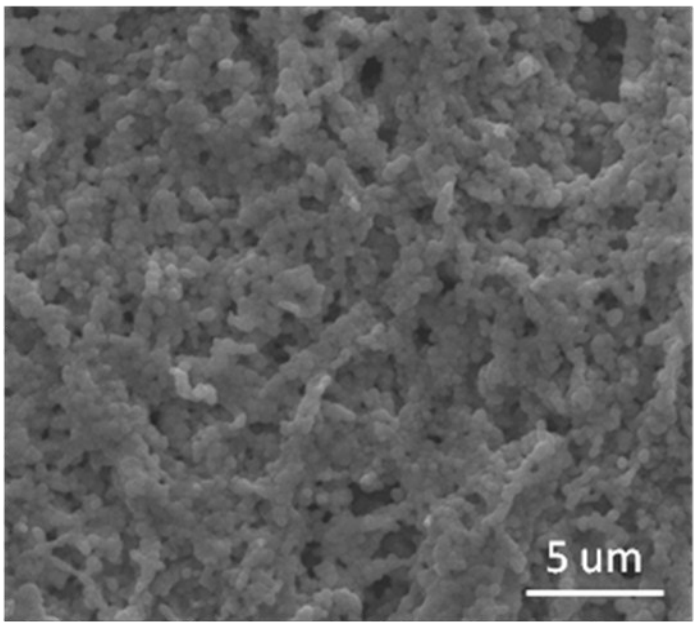

Figure S2. SEM of pure $BiVO_4$.

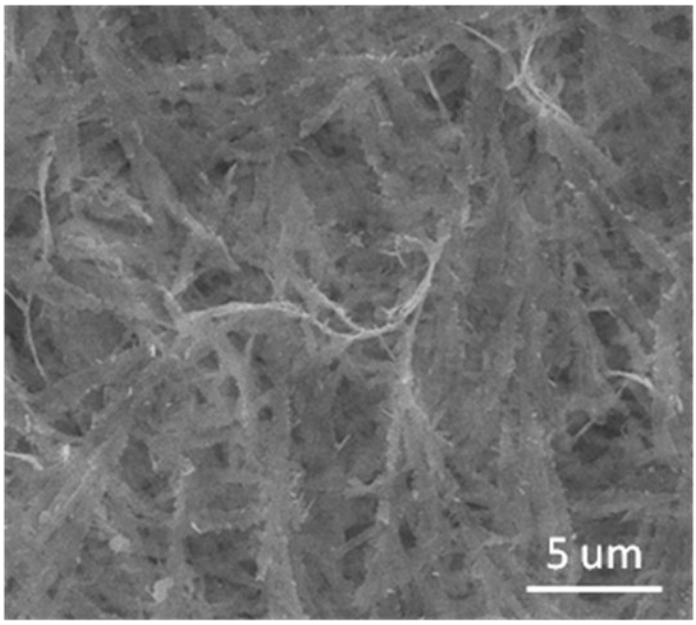

Figure S3. SEM images of pure Bi_2O_3.

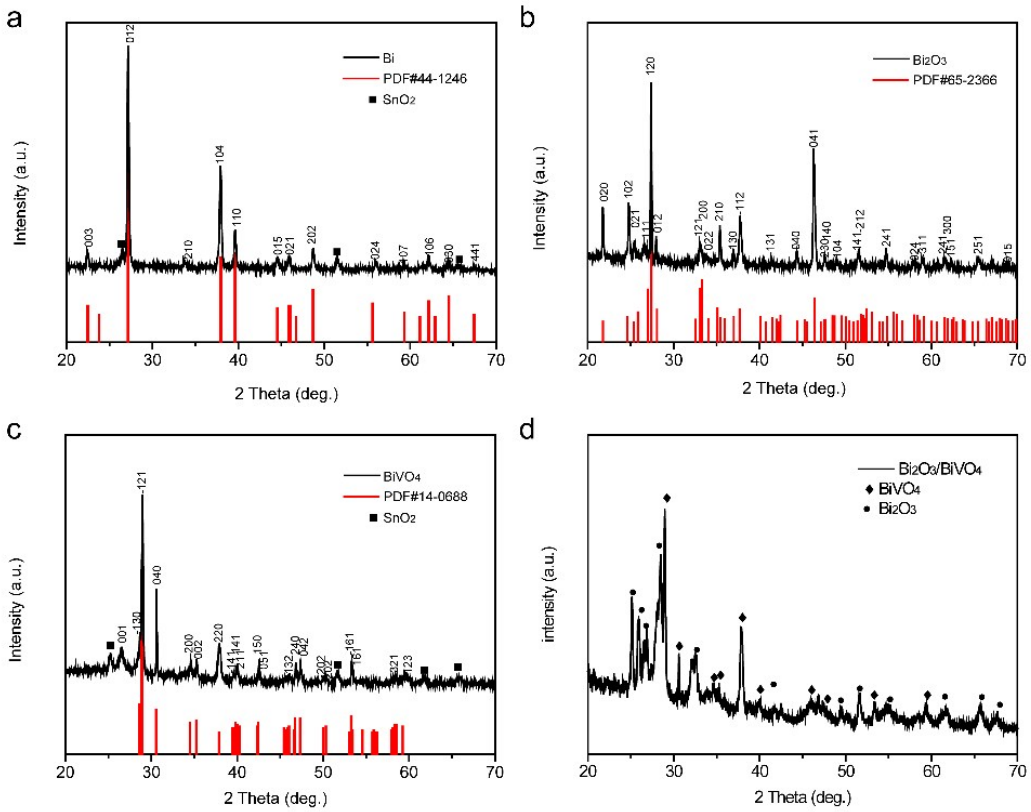

Figure S4. XRD patterns of Bi, Bi_2O_3, $BiVO_4$ and $Bi_2O_3/BiVO_4$.

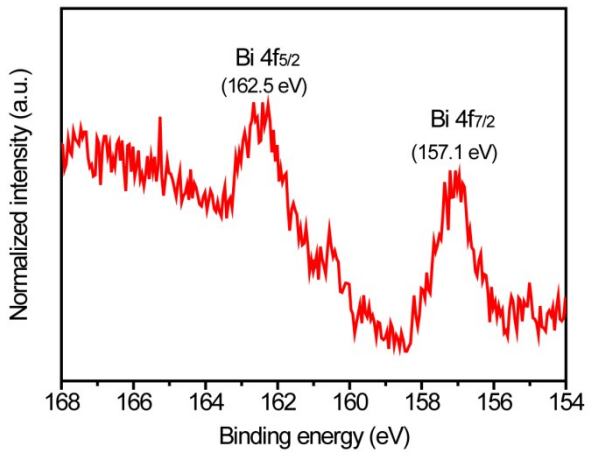

Figure S5. High-resolution Bi_{4f} XPS spectra of pristine Bi. The peaks located at 157.1 and 162.5 eV are consistent with the characteristic Bi 4*f*7/2 and Bi 4*f*5/2 of metallic Bi peaks.[1] The coarse of the Bi core level XPS spectrum is because the intensity of C 1s peak is too strong since the carbon is used as the reference in XPS measurements.

1. U. W. Hamm, D. Kramer, R. S. Zhai, D. M. Kolb, Electrochimica Acta, 1998, 43, 2969-2978.

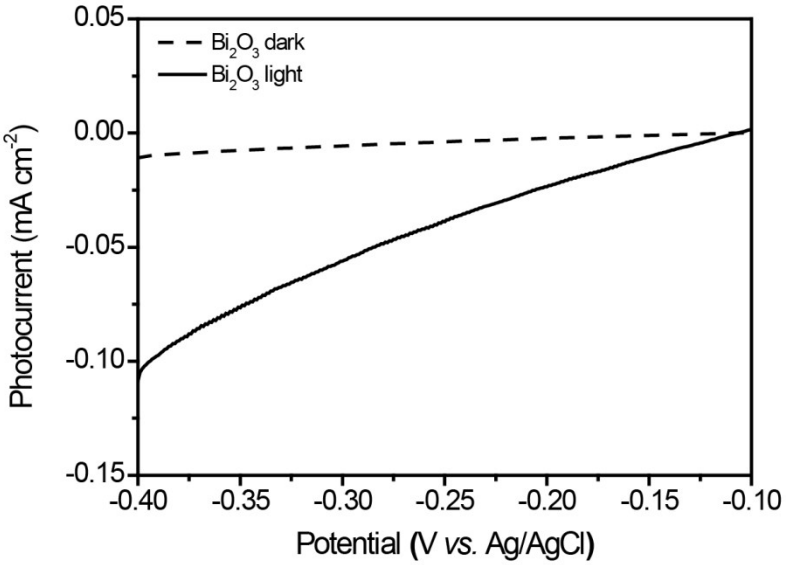

Figure S6. i-E curves of p-type Bi_2O_3.

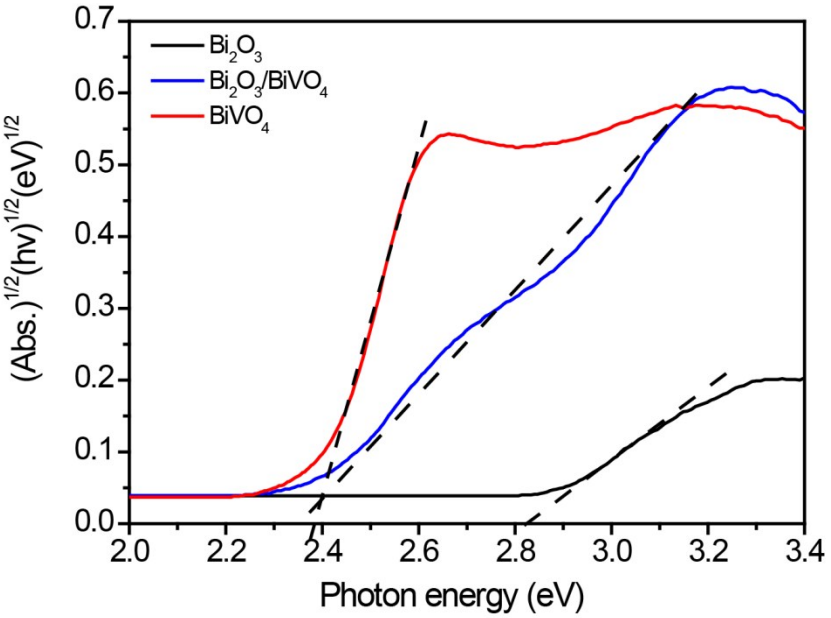

Figure S7. Plots of $(\alpha h\nu)^2$ versus the photon energy ($h\nu$) of the Bi_2O_3, $Bi_2O_3/BiVO_4$ and $BiVO_4$.

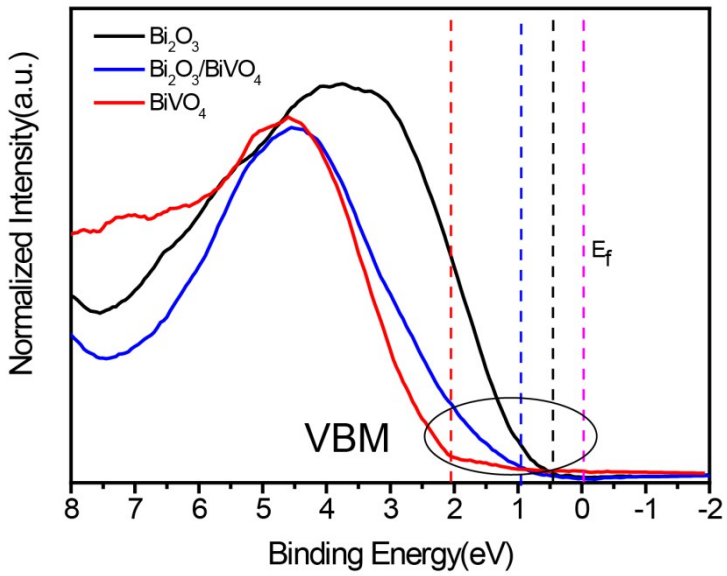

Figure S8. XPS valence band spectra of theBi_2O_3, $Bi_2O_3/BiVO_4$ and $BiVO_4$.

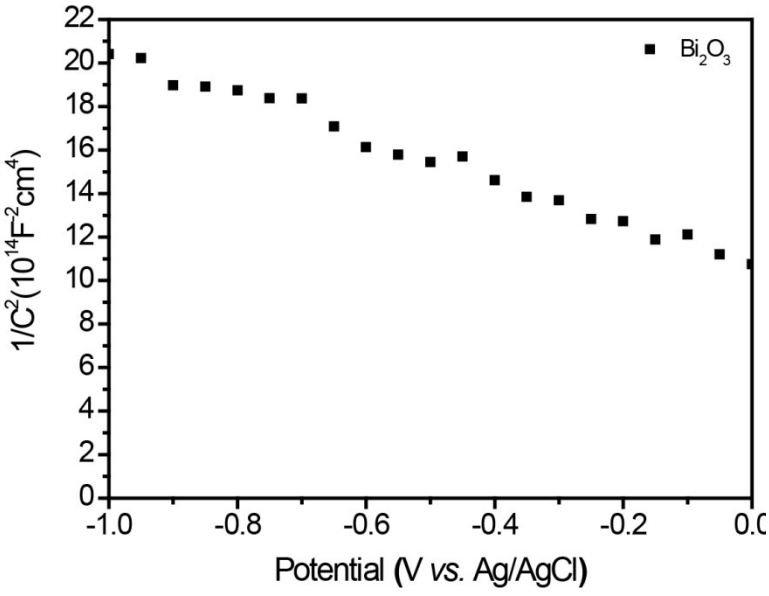

Figure S9 Mott-Schottky curves of p-type Bi_2O_3.